Environmental Sciences Europe

RESEARCH

Open Access

Spatiotemporal distribution patterns and risk characteristics of heavy metal pollutants in the soil of lead–zinc mines

Jie Cao[1,2], Cheng-yu Xie[1*] and Zhi-ru Hou[2]

Abstract

Background: The current soil environmental assessment system is inadequate in terms of the spatiotemporal distribution of heavy metal pollutants. This study employed the numerical simulation technique to predict spatiotemporal distribution patterns of heavy metals within 50 days and to assess the soil risk characteristics of heavy metal pollution near a lead–zinc mine in Hunan Province, China.

Results: The spatiotemporal distribution results indicate that the soil in the sewage plant and mining areas served as the pollution center, exhibiting a ladder-shaped pollution diffusion trend outward. When the pollution migration time reached 20 days, pollutant migration and changes tended to remain stable, high-pollution areas exhibited no drastic changes within 10 m, and low-pollution and medium-pollution areas revealed obvious changes. Moreover, the low-pollution area width approached 2 m, the depth reached 2 m, the medium-pollution area width was close to 2.5 m, and the depth approached 4 m. The percentage of areas containing lead–zinc mine soil with high to extremely high risks reached 82.88%, and extremely high-risk farmland, mining and residential areas accounted for up to 100%, 95% and 90%, respectively, of the total area. Among the pollution sources, high-risk and extremely high-risk areas in regard to heavy metal Cd accounted for 13.51 and 49.55%, respectively, of the total area.

Conclusion: This study provides new insights into the migration patterns and risk characteristics of pollutants to address soil environmental assessment system problems.

Keywords: Mine soil, Heavy metal pollution, Environmental assessment, Numerical simulation, Spatiotemporal distribution

Background

After heavy metal pollutants originating from mining activities enter soil, these heavy metals are continuously accumulated in the soil through the processes of physical and mechanical absorption, retention, colloidal physical and chemical adsorption, chemical precipitation and biological absorption [1]. When the soil capacity is exceeded, the soil composition, structure, nature and function could deteriorate [2], but heavy metals cannot be decomposed by soil microorganisms and are easily enriched in organisms [3]. Mine-contaminated land mainly involves heavy metal pollution, and heavy metal pollution evaluation encompasses a complex process and represents a worldwide problem [4]. In order to reliably evaluate heavy metal pollution various aspects need to be considered. Contaminated area analysis, pollution source determination, and spatiotemporal distribution evaluation of pollutants are essential for soil environmental assessment [5]. Soil environmental assessment can determine the risk level in the contaminated area of a given mine and thus identify pollution sources, which facilitates soil ecological remediation [6]. Heavy metal pollution can directly threaten the lives and safety of residents

*Correspondence: xiechengyu42@xtu.edu.cn
[1] College of Environment and Resources, Xiangtan University, Xiangtan 411105, China
Full list of author information is available at the end of the article

in the functional area. Hence, mine soil environmental assessment requires more attention [7].

Environmental assessment of the soil environment reflects the extent to which heavy metal pollutants are harmful to the human body, and long-term exposure to heavy metal enrichment could lead to neurological disorders and kidney failure [8]. Mass heavy metal poisoning among children in Africa has been attributed to exposure to contaminated soil originating from mines, inhalation of contaminated soil particles, and ingestion of crops grown on contaminated mine soil [9]. An environmental assessment study of a gold mine in Ghana, Africa, confirmed the above claim [10], identifying potential health risks to the local population under the influence of carcinogenic mining practices and contamination of groundwater, agricultural soil and plants, thus indicating the importance of soil environmental assessment for human health. Environmental assessment studies of soils on a global scale can be classified in three categories. The first category involves index equation-based evaluation [11–13], in which an equation is employed to project current soil heavy metal pollution conditions, thereby considering the heavy metal content, pollution differences among multiple elements and corresponding risk factors in result calculation, but this approach cannot assess the uncertainty in the prediction results. A typical soil evaluation index is the environmental index [14, 15], with objective evaluation results, which can accurately distinguish and quantify the soil risk and identify pollution sources and areas. However, this approach exhibits the disadvantage of not reflecting the spatiotemporal changes in heavy metal pollution. The second category encompasses matrix function evaluation [16–18], based on establishing an affiliation function and constructing a fuzzy relationship matrix, thereby determining the classical domain, nodal domain and coefficients to distinguish and quantify the degree of soil heavy metal pollution. However, there exist uncertainties in the factors, coefficients and matrices, the evaluation framework is thus difficult to establish, and the evaluation results are unreasonable. The third category entails geographic information evaluation [19–21], which considers spatial database information and employs remote sensing technology and geostatistics for grid establishment, resulting in training sets and spatial graphics. However, the assessment results are inaccurate, and the authenticity of the results cannot be verified. In addition, the numerical simulation technique, as a new type of mathematical model, can spatially characterize soil heavy metal pollution and incorporate temporal parameters to visualize the obtained results [22]. In the numerical simulation process of contaminated sites, Zhou et al. [23] found that pollutants were transported in soil along the direction of groundwater flow and concluded that numerical simulation could be applied to soil pollutants. Thereafter, Cao et al. [24] explored spatiotemporal distribution patterns of heavy metal pollutants in lead–zinc mine soil through numerical simulations and verified the applicability of the numerical simulation technique to heavy metal pollutants in soil.

Soil environmental assessment can reflect the degree of heavy metal damage to the environment, but cannot reflect the spatiotemporal variation characteristics of heavy metal pollution. Numerical simulations can capture soil heavy metal pollution in both two- and three-dimensional space, accurately visualize the obtained results and suitably reveal the spatiotemporal distribution of heavy metals. The application of numerical simulation technology could overcome the shortcomings of soil environmental assessment and yield more comprehensive and reliable assessment results. Therefore, this study applied the numerical simulation technique combined with environmental assessment analysis, thereby providing new insights into mine soil evaluation and providing notable support for the prevention and control of heavy metal pollutants in mine soil, in addition to risk warning.

Materials and methods

Sampling site

The study area is located in a lead–zinc mine within Hunan Province, China. The mine site exhibits a rugged terrain and variable geological structure, and many landslide disasters have occurred. The mine area is mainly dominated by red loam, followed by sandy loam (Fig. 1). The total mine area consists of six functional areas: mining area, tailings area, residential area, reclamation area, farmland area, and sewage plant area. The mining area is the functional area for ore mining and transportation [25], the tailings area is the functional area for waste ore or tailings stockpiling [26], the residential area is the functional area where local villagers live and work [27], the reclamation area is the functional area for soil ecological restoration and phytoremediation measures by the local government [28], the farmland area is the functional area for local villagers to conduct agricultural cultivation [29], and the sewage plant area is the functional area for the treatment of local mining and metallurgical wastewater and domestic sewage [30]. The present study focuses on profiling the typical heavy metals of Pb, Zn, and Cd within the soil of this lead–zinc mine.

Sampling and experimental methods

To comprehensively assess soil heavy metal pollution in the different functional areas of the mine, 20 soil sampling points were established in the reclamation area (113°04′

Fig.1 Actual view of the lead–zinc mine in Hengyang city, Hunan Province, China

07″E–113°04′30″E, 27°08′26″N–27°08′44″N), residential area (113°04′19″E–113°04′30″E, 27°08′24″N–27°08′43″N), sewage plant area (113°04′15″E–113°04′32″E, 27°08′52″N –27°08′58″N), mining area (113°04′16″E–113°04′36″E, 27°08′33″N–27°08′58″N) and tailings area (113°04′02″ E–113°04′20″E, 27°08′42″N–27°08′52″N), and eleven soil sampling points were established in the farmland area (113°04′30″E–113°04′32″E, 27°08′27″N–27°08′31″N). At each soil sampling point, 2.1 kg of soil was collected at a soil depth of 40 cm, and three replicates were obtained at each sampling point, which were mixed into one sample, placed in a sealed bag, marked, and transported to the laboratory for processing [31]. Considering the ruggedness of the mine roads and actual conditions, the sampling points were arranged via a combination of the S-based and random sampling methods for soil collection purposes [32]. The soil collected at the sampling sites was left outdoors to dry naturally for 7 days, and large sand grains and gravel particles were then separated with a 10-mesh sieve [33]. Individual samples weighed 140 g, which were dried at 104 °C for 12 h, ground, passed through a 100-mesh sieve, and thoroughly mixed in a blender [34]. The total heavy metal content was determined after the quadratic discard method was applied.

Heavy metal content assays

First, 0.5 g of mixed soil was removed via quadratic individual sampling, and the mixed soil sample was placed in a digestion tube. Dissolution of the soil samples was performed with a graphite digestion instrument. A blank group was set up during soil sample digestion, with the aim of reducing the experimental error. Certified materials (HJ/T166) were employed. The digestion process was as follows: 0.5 g of the soil sample was placed in the digestion tube, which was inserted into the digestion cavity of the graphite digestion instrument, after which a few drops of water were added for moistening. Then, 10 mL of concentrated HCl was added, and the controller was set to a low temperature (80–100 °C) for heating and evaporation until approximately 5 mL remained. Subsequently, 15 mL of HNO_3 was added, heat (100–120 °C) was applied until the sample became viscous, 10 mL of HF was added, heat (120 °C) was applied, and the ablation tube was shaken. Then, 5 mL of $HClO_4$ was added, the sample was heated (130 °C) until white smoke was emitted, and the final decomposition product was white or light yellow and viscous. After cooling, the inner wall of the tube and cap were rinsed with a dilute HNO_3 solution, the residue was dissolved under warming, and the volume was fixed to 50 mL after cooling [35, 36]. The five-point calibration method involving standard samples was implemented before heavy metals Pb, Zn and Cd were determined via flame atomic absorption spectrophotometry [37]. The slopes of the calibration curves for Pb, Zn and Cd were 0.9998, 0.9999 and 0.9997, respectively. This sample measurement approach was highly accurate and conformed to the basic standards of the JJD 694–2009 National Metrology Calibration Protocol of the People's Republic of China.

Methodology

Numerical simulation technology

COMSOL Multiphysics and MATLAB are highly advanced numerical simulation software packages. This study relied on COMSOL Multiphysics and MATLAB software to obtain numerical simulation results. Migration of heavy metal pollutants considers that the process should initially start as point pollution, spread through infiltration into surface pollution and finally reach the scope of pollution [38]. The pollution source in the numerical simulations is set to (15, − 2), and the boundary conditions of the contaminant migration behavior in soil are defined as boundaries (1), (2), and (3), of which boundary (1) is a fixed boundary, boundary (2) is the entrance, and boundary (3) is the exit.

The Richards equation [39] and governing equation for solute transport [40] were adopted to simulate the migration process of heavy metal pollutants via numerical

simulations to describe the migration changes in heavy metal pollutants in soil. Based on Eqs. (1) and (2), the migration changes in heavy metal pollutants in soil could be predicted via simulations:

$$(B + AaA)\frac{\partial C_p}{\partial t} + \nabla \cdot (-D\nabla(C_p + E)) = 0, \quad (1)$$

where B is the specific moisture capacity, Aa is the effective saturation, A is the storage coefficient, C_p is the pressure head, t is the time, D is the hydraulic conductivity, and E is the direction:

$$\frac{\partial}{\partial t}(\theta A) + \frac{\partial}{\partial t}(p_a c_a) + u \cdot \nabla A + \nabla \cdot [-\theta D_a \nabla A] = \Sigma C_a + \Sigma C_b + E_a, \quad (2)$$

where A is the concentration, p_a is the bulk density, C_a is the weight, θ is the porosity, D_a is the hydrodynamic dispersion tensor, C_a is the reaction in water, C_b is the reaction solute, and E_a is the solute per unit time.

Environmental risk assessment methodology

Rapant et al. [41] proposed the environmental risk index method to characterize the environmental risk in contaminated environments, which specifies corresponding environmental risk classification criteria and can quantitatively measure the environmental risk level of soil contaminated with heavy metals. Based on Eqs. (3) and (4), the environmental risk of heavy metal pollutants in soil can be calculated.

$$I_{ERi} = (AC_i/RC_i) - 1 \quad (3)$$

$$I_{ER} = \sum_{i=1}^{n} I_{ERi}, \quad (4)$$

where I_{ERi} is the environmental risk index of the ith element at the supercritical limit, AC_i is the analytical content of the ith element, RC_i is the critical limit of the ith element, and I_{ER} is the environmental risk of the test sample.

The environmental risk index method distinguishes 5 risk levels: $I_{ER} \leq 0$, level 1—no risk; $0 < I_{ER} \leq 1$, level 2—low risk; $1 < I_{ER} \leq 3$, level 3—medium risk; $3 < I_{ER} \leq 5$, level 4—high risk; $I_{ER} > 5$, level 5—extremely high risk.

The functional area risk index division is as follows: reclamation area (number: 1–20), residential area (number: 21–40), sewage plant area (number: 41–60), mining area (number: 61–80), tailings area (number: 81–100), and farmland area (number: 100–111). Based on Eq. (5), the functional area risk index mean of heavy metal pollutants in soil can be calculated:

$$Mean = \frac{X_1 + X_2 + \cdots + X_n}{n}. \quad (5)$$

Results and analysis

Environmental risk assessment

The mean value of the environmental risk index for the three heavy metals in the sampled mine soil exhibited the order of Pb (7. 57) > Cd (6. 60) > Zn (5. 51) > 5, and the I_{ER} value reached 19.68 > 5. Hence, each of the three heavy metals posed a very high risk, indicating that these three heavy metals generated severe compound pollution, and during soil remediation, joint treatment of the above three heavy metals should be considered (Fig. 2). The tested mine soil as a whole occurred at a very high environmental risk level, indicating that the enrichment impact on the surrounding soil after years of high-intensity mineral resource remining and smelting activities in the mine was significant and required soil pollution prevention and control as soon as possible [42].

The mean soil environmental risk index for each functional area of the mine was as follows: mining area (49.24) > sewage plant area (18.65) > tailings area (17.94) > farmland area (15.46) > residential area (10.23) > 5 > reclamation area (4.69) > 3 (Table 1). These results demonstrate that the mining, sewage plant, tailings, farmland, and residential areas all occurred at the extremely high environmental risk level. Among the various functional areas of the mine, the environmental risk index for the mining area was several times that for the other areas, indirectly reflecting that the heavy metal pollution level in the soil of the mining area was extremely high, which is directly related to the mining activities in the mining area, including unregulated ore collection, smelting, rock weathering and reckless accumulation of waste rock tailings. This could lead to direct infiltration of heavy metal pollutants into the soil under migration [43]. The reclamation area exhibited a high environmental risk, which indicates that the local government should achieve a better ecological restoration effect in land reclamation and restoration.

In terms of the soil environmental risk level, the proportions of the risk-free, low-risk, medium-risk, high-risk, and extremely high-risk mine areas reached 8.11%, 4.50%, 4.50%, 6.31%, and 76.58%, respectively, of the total area. Areas with a high risk and above accounted for 82.88% of the total area, which constitutes a notable environmental warning signal to surrounding residents, and soil remediation of the mine site should be carried out as soon as possible (Table 2). Extremely high-risk farmland areas occupied 100% of the soil in the

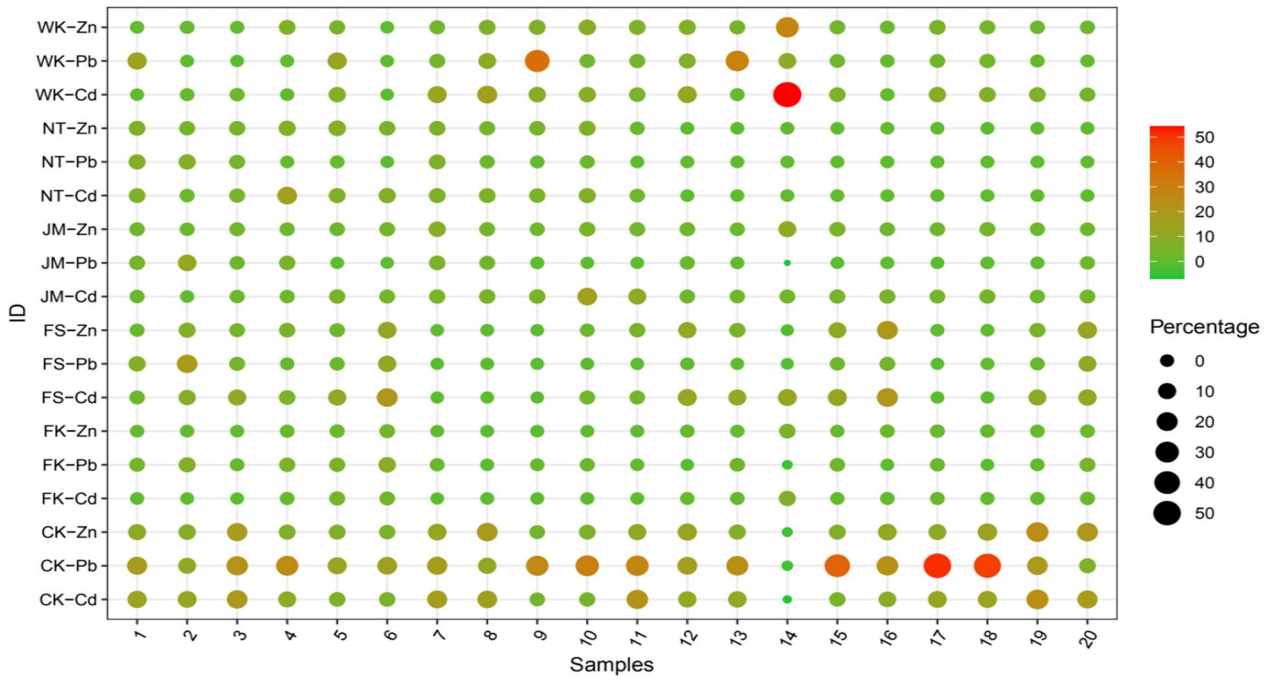

Fig.2 Environmental risk index for the heavy metals in the different mine functional areas. WK (tailings area), NT (farmland area), JM (residential area), FS (sewage plant area), FK (reclamation area), CK (mining area)

Table 1 Environmental risk index for the different functional areas of the mine

Functional number	Reclamation area	Residential area	Sewage plant area	Mining area	Tailings area	Farmland area
1	6.67	14.87	19.34	64.61	22.98	30.21
2	10.34	20.90	49.26	44.31	3.70	20.81
3	0.43	6.86	14.54	48.09	1.92	11.04
4	6.04	7.73	9.08	32.82	5.17	18.52
5	16.42	10.75	23.56	36.86	38.00	24.18
6	12.66	5.82	35.81	21.74	-1.49	10.07
7	0.49	15.58	-2.38	39.72	18.34	15.56
8	− 0.33	12.95	− 1.24	44.65	31.61	12.18
9	0.27	7.37	− 2.16	30.54	47.68	10.17
10	1.49	16.06	3.72	33.33	15.65	12.23
11	− 0.24	14.44	8.19	64.92	17.12	5.08
12	0.94	7.48	19.61	33.17	21.75	
13	7.26	7.87	22.01	65.61	53.22	
14	1.12	0.93	1.36	− 2.10	13.00	
15	4.37	9.98	28.11	59.47	14.36	
16	3.89	12.31	72.21	71.67	5.69	
17	4.01	4.65	− 0.96	53.38	12.14	
18	1.32	8.82	− 1.01	73.59	13.85	
19	4.91	7.70	24.46	105.69	14.43	
20	11.71	11.53	49.47	62.68	9.68	

Table 2 Environmental risk level in the different functional areas of the mine

Level	Total mine area (%)	Reclamation area (%)	Residential area (%)	Sewage plant area (%)	Mining area (%)	Tailings area (%)	Farmland area (%)
1	8.11	10	0	25	5	5	0
2	4.50	20	5	0	0	0	0
3	4.50	15	0	5	0	5	0
4	6.31	20	5	5	0	5	0
5	76.58	35	90	65	95	85	100

different functional areas. This phenomenon is closely related to the nature of soil in these farmland areas. The soil in these farmland areas belongs to clay soil with a high water content, in which heavy metal elements can easily accumulate [44]. In addition, under rainwater runoff, many pollutants are transported from the top of hills and subsequently accumulate in farmland areas [45]. Extremely high-risk mining areas accounted for 95%, extremely high-risk residential areas occupied 90%, extremely high-risk tailings areas accounted for 85%, extremely high-risk sewage plant areas occupied 65%, and extremely high-risk reclamation areas accounted for 35% of the total area, which indicates that the impact of the different production activities on heavy metal accumulation in soil was differentiated and priority should be given to the treatment and maintenance of farmland areas [46].

Prevention and control of soil environmental pollution should first determine the risk source areas and heavy metal risk sources for priority control determination. According to physical examination, most residents living near lead–zinc mines suffer certain diseases, which are directly related to heavy metals Pb, Zn and Cd in lead–zinc mine soil. Heavy metals Pb, Zn and Cd in the soil of the mining area indicate extremely high pollution levels, with risks reaching as high as 95, 80 and 80%, respectively, thus confirming that mining activities in the mining area can cause serious compound pollution in the soil environment within the region, which is highly difficult to manage (Table 3). Therefore, the mining area

Table 3 Environmental risk levels of the different heavy metals in the various functional mine areas

Level	Reclamation area			Residential area			Sewage plant area		
	Pb (%)	Zn (%)	Cd (%)	Pb (%)	Zn (%)	Cd (%)	Pb (%)	Zn (%)	Cd (%)
1	20	20	35	40	0	0	45	25	25
2	20	30	25	20	0	10	10	5	0
3	20	45	35	10	30	20	10	15	10
4	15	5	0	20	60	35	10	10	10
5	25	0	5	10	10	35	25	45	55
Level	**Mining area**			**Tailings area**			**Farmland area**		
	Pb (%)	**Zn (%)**	**Cd (%)**	**Pb (%)**	**Zn (%)**	**Cd (%)**	**Pb (%)**	**Zn (%)**	**Cd (%)**
1	5	5	5	15	5	10	18.18	0.00	0.00
2	0	0	0	10	10	5	18.18	0.00	0.00
3	0	0	5	25	10	20	27.27	9.09	0.00
4	0	15	10	20	40	0	9.09	45.45	36.36
5	95	80	80	30	35	65	27.27	45.45	63.64
Level			**Total mine area**						
			Pb (%)			**Zn (%)**			**Cd (%)**
1			24.32			9.91			13.51
2			12.61			8.11			7.21
3			14.41			18.92			16.22
4			12.61			27.93			13.51
5			36.04			35.14			49.55

should be prioritized as a risk source area [47]. The soil environmental risk levels in the sewage plant area, tailings area, farmland area, residential area, and reclamation area were highly variable, indicating that the soil in the mining area suffered great damage due to human factors and was contaminated to notably different degrees based on the different areas. Consequently, an uneven soil pollution distribution was observed [48]. The high-risk and extremely high-risk heavy metal pollution source areas in regard to the occurrence of Pb, Zn, and Cd in the mine soil accounted for 12.61 and 36.04%, 27.93 and 35.14%, and 13.51 and 49.55%, respectively, of the total area. Via comparison of the sources of these three heavy metal pollutants, it could be concluded that Cd contamination of the soil in the mining area was the most serious and that the study area was contaminated by Cd with the highest soil environmental risk coefficient. Moreover, the contaminated area was very extensive, the degree of contamination was high, and the toxic risk to humans occurred at a high level [49]. Therefore, according to the ranking of the soil pollution risk sources, i.e., Cd > Zn > Pb, heavy metal Cd should be considered the highest-priority soil pollution risk source for control in the study area.

Environmental risk spatial distribution prediction model

The spatial distribution of pollutants is an important method to reveal the risk of soil environmental pollution. There were mainly three high-pollution risk areas distributed in the north and east. The mine pollution distribution was concentrated, and the pollution trend basically exhibited an 8-type pattern (Fig. 3). The soil in the northern sewage treatment plant area and eastern mining area was highly polluted, and treatment and maintenance measures should be implemented in advance to prevent pollution migration from impacting the surrounding soil after the emergence of high soil environmental risks. The overall pollution situation demonstrated that the mining area exhibited a peak, there occurred abnormally high values, and the surrounding distribution revealed a gradually decreasing trend, indicating that production activities affected the accumulation of heavy metals in the mining area. Hence, it is necessary to rectify and plan human activities and the development and utilization of mineral resources in the mining area [50]. The

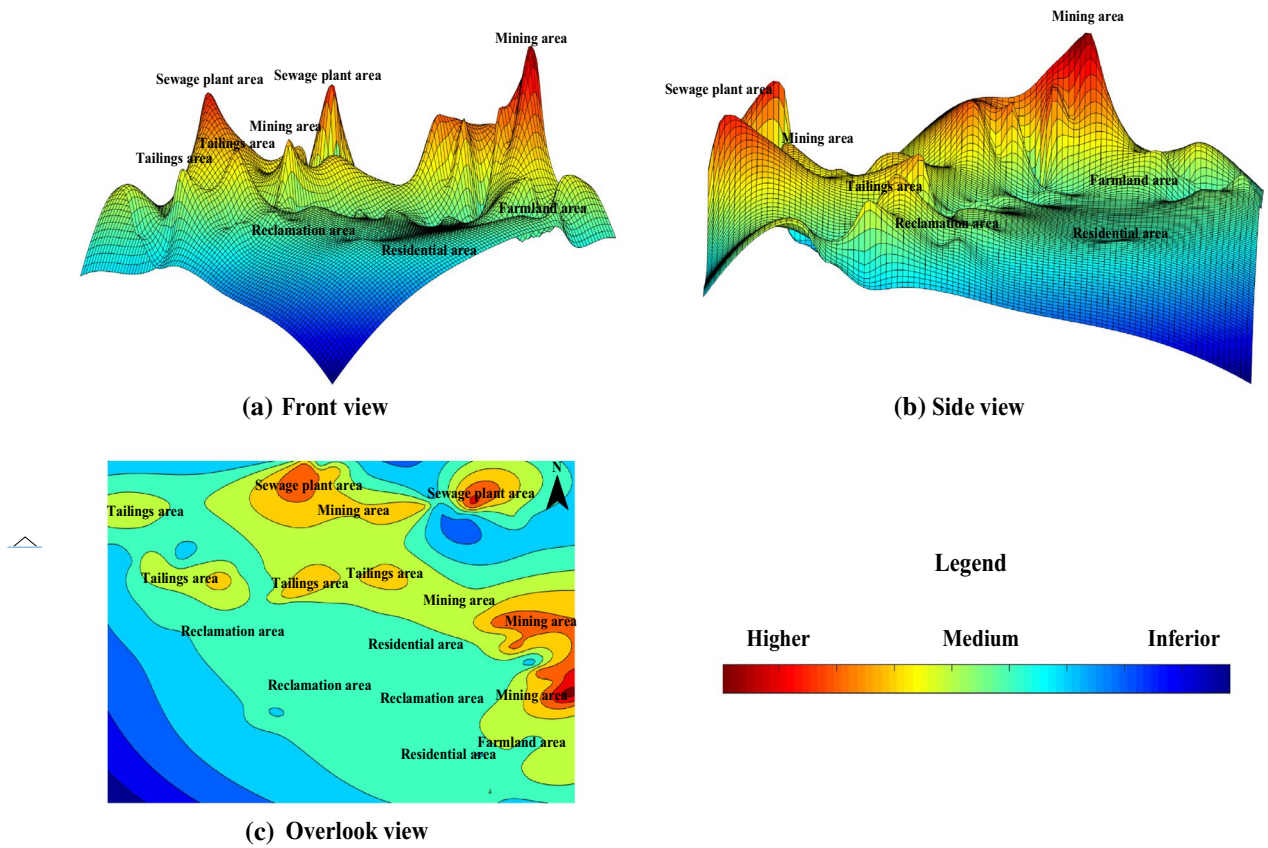

Fig. 3 Three-dimensional map of the environmental risk levels of the heavy metal pollutants in the different areas of the mine

sewage plant area, mining area and tailings area pollution distributions are closely linked, the heavy metal pollution distribution within the region is relatively concentrated, and there exist differences in the pollution distribution. It could be found that these three areas served as the pollution center, while the surrounding pollution level exhibited a gradual weakening trend, which could lead to pollution penetration and diffusion in the different functional areas within the mine. This indicates that the pollution sources between these three areas are consistent and significantly correlated, which is related to early unreasonable mineral resource development, tailings piling and other highly correlated anthropogenic activities [51]. In addition, there occurs mutual contamination between mining, tailing and sewage disposal activities within the mine, thus altering the status of soil contamination between the different regions.

The soil in the sewage plant area exhibited two highly polluted blocks, while the center of pollution coincided with the center of the area, indicating wave-like outward extension. Most of the surrounding soil exhibited a step-type pollution distribution. On the one hand, this could be attributed to the unregulated discharge of smelting wastewater by sewage plants [52], while on the other hand, this could also be attributed to the improperly managed sewage plant drainage system [53], which indicates that the sewage plant severely polluted the surrounding soil, and sewage treatment measures should be implemented to prevent heavy metal pollution upon migration through water after diffusion. There were similar contamination distributions between the reclaimed and residential areas in the southern part of the mine, with a moderate risk of contamination, and these two areas are adjacent to the mining and tailings areas, thus confirming that the mining and tailings areas of the mine exerted a fundamental impact on the soil in adjacent areas. Therefore, effective soil contamination prevention and control of pollution sources in the mining and tailings areas could eliminate the associated pollution attributed to soil pollution migration and reduce the risk of pollution in the surrounding functional areas [54]. In addition, the large differences in soil pollution status between the different functional areas suggest that the variability in human activities in the different areas considerably influenced the degree of soil heavy metal accumulation.

Spatiotemporal distribution prediction model

The migration mechanism of heavy metal pollutants within mine soil entails a dynamic process [55], and the spatiotemporal distribution of heavy metal pollutants within soil can be addressed by applying simulation technology with the aim of exploring migration changes in heavy metal pollutants. During the migration process, heavy metal pollutants initially infiltrate into the soil from boundary (2) and continue to diffuse toward boundary (3) due to gravity and soil pore water transport, and the pollution diffusion direction near boundary (1) demonstrates a vertical diffusion trend, which is directly related to the angle of the mine soil slope (Fig. 4). In the vertical state, heavy metal pollutants in soil could appear to accumulate unilaterally, but the pollution infiltration

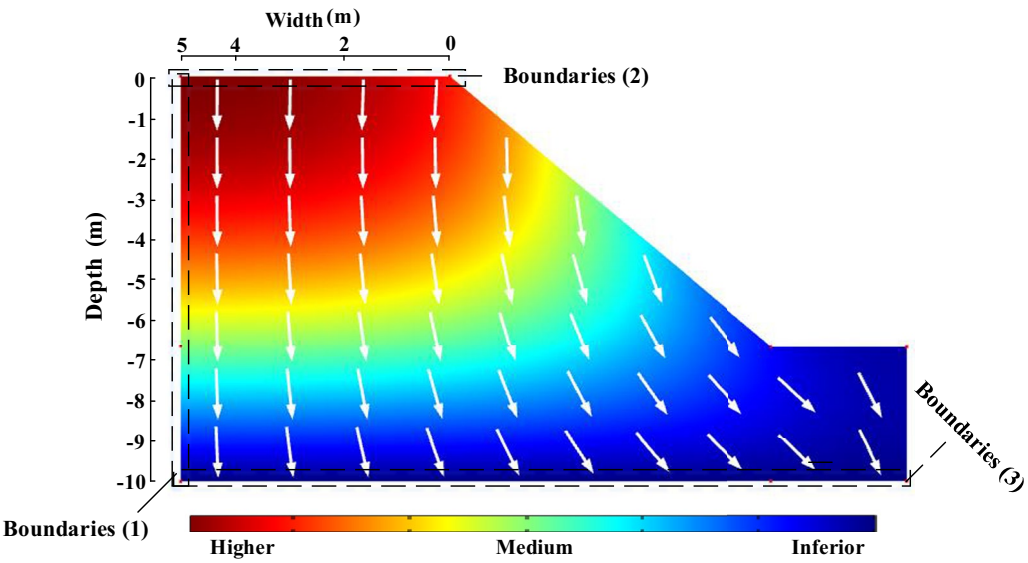

Fig. 4 Transport directions of the heavy metal pollutants

direction remains oriented from the high-pollution area to the low-pollution area during migration [56]. In addition, based on the pollution migration direction between boundaries (2) and (3), it can be concluded that pollutant migration also exhibits the characteristic of diffusion along multiple lateral directions, which can be summarized as diffusion from the polluted side toward the right hemisphere, which is consistent with the conclusion of Jacques et al. [57] that the diffusion direction of heavy metal pollutants could exhibit irregular dispersal movement along all directions with increasing soil depth, but the change trend of pollutant infiltration always exhibits a semielliptical shape during migration.

The spatiotemporal distribution of heavy metal pollutants in the mine soil was investigated (Fig. 5), which revealed the following: on day zero, the heavy metal pollutants gathered at the pollution source, the surface width reached 1 m, and no pollution infiltration changes occurred. On the 1st day, the heavy metal pollutants started to migrate, the pollutants gradually infiltrated, the high-pollution area width reached 2 m, the depth reached 3 m, and the pollution sources exhibited the low-pollution phenomenon, which confirms the theory that pollutants can continuously infiltrate into soil [58]. On the 2nd day, heavy metal pollutant migration drastically changed, with a high-pollution area width of 4 m and a depth of 4 m. On the 5th day, the migration rate of the heavy metal pollutants continuously increased, and the width of the highly contaminated area reached 2.5 m. However, if the width of the boundary was not set in the model, the width of this contaminated area could exceed the limit, and the depth could approach 6 m. On the 10th day, the migration capacity of the heavy metal pollutants reached its peak, the depth of the highly polluted area already exceeded 10 m, and the pollution source area gradually became a low-risk area. On the 15th day, with continuous downward movement of pollutants, the low-pollution area also expanded, with a width close to 1.5 m and a depth close to 1.5 m, indicating that if the subsequent environmental pollution could be controlled, the surface layer would not further expand. On the 20th day, the pollutant migration trend reached the steady state, no drastic change in the high-pollution area occurred within 10 m, obvious changes were observed in the low- and medium-pollution areas, the width of the low-pollution area approached 2 m, the depth was close to 2 m, the width of the medium-pollution area almost reached 2.5 m, and the depth approached 4 m. The 25th day was similar to the 20th day, which suggests that the spatiotemporal distribution of the pollutants within 10 m already approached the stable state and could not further produce large fluctuations without subsequent pollution [59]. To verify the validity of this statement, a 50 day numerical simulation experiment was carried out, and the final verification results were consistent. The migration trends on the 50th day were the same as those on the 25th day, confirming that the migration process of heavy metal pollutants within the 10 m depth approached stability, and the spatiotemporal distribution of the three pollution levels of high, medium and low risks did not significantly differ from that on the 20th day.

At the temporal level, the transport process of heavy metal pollutants in soil was enhanced with increasing number of days, from day zero to the 5th day. The migration trend of pollutants was very obvious, spreading outward in a semicircular wave, and a high soil pollution level always occurred within the depth range of 4 m, which indicates that the transport capacity of pollutants greatly fluctuated at the initial stage. Moreover, if the pollution sources could be controlled during this period, the pollution infiltration area could be greatly reduced. From the 10th day to the 15th day, the change trend of the pollutants gradually weakened, and the pollution depth exceeded 10 m, but the low-pollution area also continued to expand during pollutant infiltration. A pollution accumulation surface was often generated in the deep layers, and only a small fraction accumulated in surface soil [60]. This phenomenon indicates that groundwater could also suffer from serious heavy metal pollution. From the 15th day to the 20th day, the pollutant migration change trend approached stability, there occurred no drastic response fluctuations in the high-pollution area, and the distribution of low- and medium-pollution areas expanded to the 3.5 m depth. Therefore, 20 days could be adopted as a time node for pollution migration, and pollution sources should be identified and then mitigated within 20 days during pollution source control to avoid greater environmental pollution. From the 20th day to the 25th day, the migration change in pollutants was similar to that on day 20. At this time, two speculations could be made. First, the migration behavior of the pollutants reached the stable stage, and 20 days could be regarded as a turning point for migration capacity stabilization. Second, when pollutant migration exceeds a soil depth of 10 m, pollutants could continue to migrate downward, and pollution changes could continue [61]. There exists a specific period ranging from 20 to 25 days. By studying the period from 25–50 days, validation revealed that when the simulation time was extended by 25 days, the migration behavior of pollutants always exhibited a high similarity to that on day 25. Therefore, day 20 was the turning point in regard to stabilization of the migration capacity, but this did not indicate that pollution infiltration had

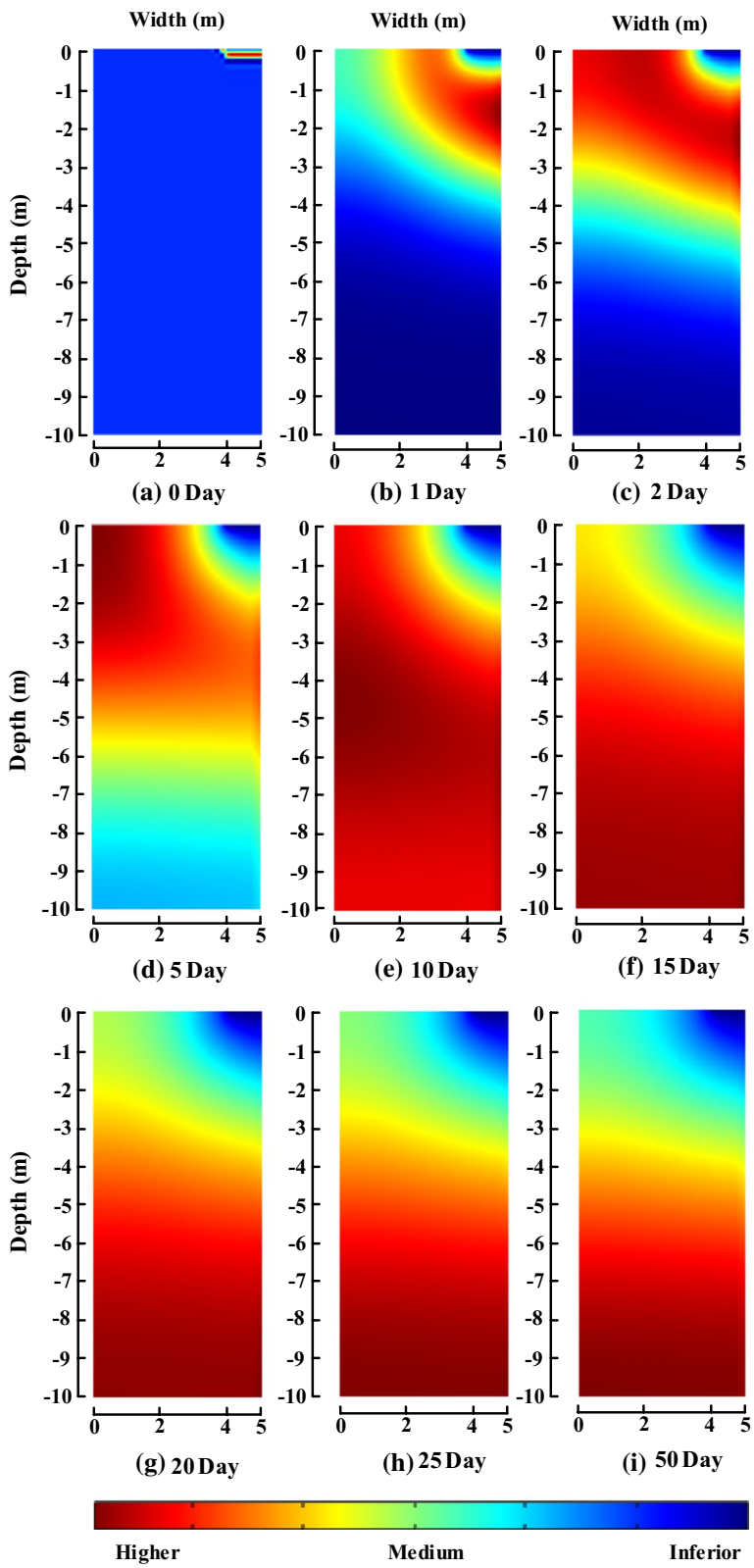

Fig. 5 Spatiotemporal distribution of the heavy metal pollutants. The color legend applies to the whole diagram; the left side shows the high-pollution area, and the right side shows the low-pollution area

ceased, and the heavy metal pollutants in soil could still affect a larger area of soil for a considerable period.

At the spatial level, there occurred three stages, namely, before, during and after, and the first stage involved a high-risk area with a depth ranging from 0–3 m. The contamination level of heavy metal pollutants in the surface layer was serious, the soil ecological risk was extremely high, and soil control is needed targeting surface soil to prevent local residents from being harmed through the food chain [62]. In the medium term, the depth range from 3 to 10 m represented the high-risk area, and the pollution level in the middle soil layer was higher than that in the surface soil. To more effectively remediate this risk area, plants with a root system larger than 3 m should be selected as the first choice for mine soil remediation [63]. Later, when the high-risk area exceeds the 10 m depth, heavy metal pollution further infiltrates into the deep soil. When pollution reaches the deep soil, groundwater is very easily contaminated, which could lead to serious contamination of surrounding water sources [64]. Therefore, to effectively control pollution, it is necessary to control pollution infiltration in the medium term to prevent pollution expansion. Heavy metal pollutants diffuse from the source to surrounding areas in soil, and the percolation path can continuously change in the soil space and erratically diminish with increasing depth [65], but the soil at the different depth levels could exhibit varying pollutant migration behaviors due to the difference in soil texture and soil pore space [66]. The migration ability of heavy metal pollutants in the range from 4 to 6 m was obviously weakened, and the migration ability and pollution level were also much lower than those in the depth range from 0 to 4 m, which indicates that the infiltration rate of soil pollutants could decrease with increasing depth in the migration process of heavy metal pollutants, thus causing pollutants to gather in the middle soil layer. It could be inferred that when the depth exceeds 10 m, the migration ability of heavy metal pollutants relative to the 0–4 m depth could demonstrate a significant weakening trend, and the pollution level could continue to decrease. This is consistent with the results of Černík et al. [67], who found that the migration capacity of heavy metal pollutants is mainly influenced by convection, diffusion and dispersion, with the ranking of the pollution magnitude in the order of middle soil layer > surface soil layer > deep soil layer.

Migration of heavy metal pollutants involves a continuous seepage process, and heavy metal pollutants in soil can be regarded as solutes, which can continuously seep downward under certain external conditions [68]. The spatiotemporal distribution of soil heavy metals revealed that most pollutants accumulated in the middle soil layer at depths from 3 to 10 m. The migration change ability from 0 to 3 m was notable, but the pollution distribution was narrow, and at depths beyond 10 m, the heavy metal pollutant migration capacity decreased, and the pollution level also gradually decreased with increasing soil depth. It was concluded that most heavy metal pollutants in the soil accumulated at depths from 3 to 10 m, with less contamination at depths from 0 to 3 m, which indicates that the ecological risk level in the middle soil layer could be higher than that in the surface soil layer, and long-root plants should be cultivated to mitigate the environmental pollution encountered in the area [69] and reduce the soil environmental risk.

Conclusion

Improving the soil environment evaluation system is crucial for early warnings and prevention and control of heavy metal pollution problems. This study applied the environmental risk index to analyze pollution sources and pollution areas, proposed the integration of the numerical simulation technique to further explore the spatiotemporal distribution patterns of heavy metal pollutants and revealed the hazard level and associated risk control measures for the soil in each functional area within the lead–zinc mine. The research route differed from previous single-factor environmental assessment studies of soil, but numerical simulation and predictive analysis were employed to further improve the assessment system and comprehensively reveal the pollution risk and spatiotemporal distribution characteristics of lead–zinc mines.

The soil I_{ER} value in the total mine area reached 19.68 > 5, which indicates a very high environmental risk level and requires soil pollution prevention and control as soon as possible. The soil I_{ER} value in the mining area reached 49.24, the heavy metal pollution sources of Pb, Zn and Cd in the functional area indicated extremely high pollution levels, and the mining area should be given priority as a risk source area. The soil pollution risk sources were ranked as Cd > Zn > Pb, and heavy metal Cd should be considered a priority source of soil contamination risks for control in the study area.

There mainly occurred three high-pollution risk areas in the mine, distributed in the north and east. The mine pollution distribution was concentrated, and the pollution trend basically exhibited an 8-type pattern. The overall pollution conditions revealed the mining area as the peak area. There were abnormally high values, and the surrounding distribution exhibited a gradually decreasing trend. Treatment and maintenance measures should be implemented in advance to avoid high soil environmental risks after the migration of contaminants from surrounding soil.

The 20th day was identified as a turning point in regard to stabilization of the migration capacity. In pollution source control, pollution sources should be identified and then mitigated within 20 days to avoid greater environmental pollution, but this does not suggest that pollution infiltration has ceased, and heavy metal pollutants in soil could still affect a large area of soil for a considerable period.

Most heavy metal pollutants in the soil accumulated and were distributed at depths from 3 to 10 m, but the contamination distribution was narrow at depths from 0 to 3 m, which indicates that the ecological risk level in the middle soil layer could be higher than that in the surface soil, and long-root plants should be cultivated to mitigate environmental pollution in this area and reduce the soil environmental risk.

Numerical simulation technology methods are suitable for the prediction of the spatiotemporal distribution of soil heavy metal pollutants. However, soil samples are difficult to collect at depths from 3 to 10 m for quantitative verification of simulation results, so it is necessary to collect soil samples at depths from 3 to 10 m for subsequent scientific research on prediction verification.

Acknowledgements
The authors wish to give special thanks to Ms. ZHANG Kang for her careful guidance of the experiments. We would like to thank Mr. DAI Huangbiao of the Hunan Pengyuan-Hongda Mining Company for his help with sample collection.

Authors' contributions
CJ planned and designed the study. CJ conducted all the experiments. CJ performed the laboratory analysis. CJ and HZR performed the data analysis. XCY was the funding provider for this article. The manuscript was written by CJ, XCY and HZR commented on previous versions of the manuscript. All authors read and approved the final manuscript.

Funding
This research was funded by the Natural Science Foundation of Hunan Province, grant number 2021JJ30679, and the Hunan Provincial Department of Education General Project, grant number 19C1744.

Availability of data and materials
The data analyzed in the current study are available from the corresponding author upon reasonable request.

Declarations

Ethics approval and consent to participate
Not applicable.

Consent for publication
Not applicable.

Competing interests
The authors declare that they have no known competing personal interests or relationships that could have appeared to influence the scientific work in this manuscript.

Author details
[1]College of Environment and Resources, Xiangtan University, Xiangtan 411105, China. [2]School of Metallurgy and Environment, Central South University, Changsha 410083, China.

Received: 28 December 2021 Accepted: 8 March 2022
Published online: 19 March 2022

References

1. Montalván-Olivares DM, Santana CS, Velasco FG, Luzardo FHM, Andrade SFR, Ticianelli RB, Armelin MJA, Genezini FA (2021) Multi-element contamination in soils from major mining areas in Northeastern of Brazil. Environ Geochem Health 43(11):4553–4576. https://doi.org/10.1007/s10653-021-00934-x
2. Zhao XL, He BH, Wu HY, Zheng GD, Ma XX, Liang JJ, Li P, Fan QH (2020) A comprehensive investigation of hazardous elements contamination in mining and smelting-impacted soils and sediments. Ecotoxicol Environ Saf 192:110320. https://doi.org/10.1016/j.ecoenv.2020.110320
3. Akopyan K, Petrosyan V, Grigoryan R, Melkomian DM (2018) Assessment of residential soil contamination with arsenic and lead in mining and smelting towns of northern Armenia. J Geochem Explor 184:97–109. https://doi.org/10.1016/j.gexplo.2017.10.010
4. Díaz-Morales DM, Erasmus JH, Bosch S, Nachev M, Smit NJ, Zimmermann S, Wepener V, Sures B (2021) Metal contamination and toxicity of soils and river sediments from the world's largest platinum mining area. Environ Pollut 286(335):117284. https://doi.org/10.1016/j.envpol.2021.117284
5. Kim DM, Kwon OH, Oh YS, Lee JS (2021) Determination of soil contamination sources in mining area using Zn/Cd ratios with mobile Cd. Environ Geochem Health 43(10):4061–4074. https://doi.org/10.1007/s10653-021-00820-6
6. Hadzi GY, Ayoko GA, Essumang DK, Osae SKD (2019) Contamination impact and human health risk assessment of heavy metals in surface soils from selected major mining areas in Ghana. Environ Geochem Health 41(6):2821–2843. https://doi.org/10.1007/s10653-019-00332-4
7. Wang L, Yang D, Li ZT, Fu YH, Liu XM, Brookes PC, Xu JM (2019) A comprehensive mitigation strategy for heavy metal contamination of farmland around mining areas—screening of low accumulated cultivars, soil remediation and risk assessment. Environ Pollut 245:820–828. https://doi.org/10.1016/j.envpol.2018.11.062
8. Candeias C et al (2011) Assessment of soil contamination by potentially toxic elements in the aljustrel mining area in order to implement soil reclamation strategies. Land Degrad Dev 22(6):565–585. https://doi.org/10.1002/ldr.1035
9. Gzik A, Kuehling M, Schneider I, Tschochner B (2003) Heavy metal contamination of soils in a mining area in South Africa and its impact on some biotic systems. J Soils Sediments 3(1):29–34. https://doi.org/10.1007/BF02989466
10. Bempah CK, Ewusi A (2016) Heavy metals contamination and human health risk assessment around Obuasi gold mine in Ghana. Environ Monit Assess 188(5):1–13. https://doi.org/10.1007/s10661-016-5241-3
11. Dogra N, Sharma M, Sharma A, Keshavarzi A, Minakshi BR, Thukral AK, Kumar V (2020) Pollution assessment and spatial distribution of roadside agricultural soils: a case study from India. Int J Environ Health Res 30(2):146–159. https://doi.org/10.1080/09603123.2019.1578865
12. Marrugo-Negrete J, Pinedo-Hernández J, Díez S (2017) Assessment of heavy metal pollution, spatial distribution and origin in agricultural soils along the Sinú River Basin, Colombia. Environ Res 154:380–388. https://doi.org/10.1016/j.envres.2017.01.021
13. Wieczorek J, Baran A, Urbański K, Mazurek R, Klimowicz-Pawlas A (2018) Assessment of the pollution and ecological risk of lead and cadmium in soils. Environ Geochem Health 40:2325–2342. https://doi.org/10.1007/s10653-018-0100-5
14. Ghanavati N, Nazarpour A, De-Vivo B (2019) Ecological and human health risk assessment of toxic metals in street dusts and surface soils in Ahvaz,

Iran. Environ Geochem Health 41(2):875–891. https://doi.org/10.1007/s10653-018-0184-y
15. Ustaoğlu F (2021) Ecotoxicological risk assessment and source identification of heavy metals in the surface sediments of Çömlekci stream, Giresun, Turkey. Environ Forensics 22(1–2):130–142. https://doi.org/10.1080/15275922.2020.1806148
16. Agyeman PC, Ahado SK, John K, Kebonye NM, Vašát R, Borůvka L, Kočárek M, Němeček K (2021) Health risk assessment and the application of CF-PMF: a pollution assessment-based receptor model in an urban soil. J Soils Sediments 21(9):3117–3136. https://doi.org/10.1007/s11368-021-02988-x
17. Dimitrov DS, Nedyalkova MA, Donkova BV, Simeonov VD (2019) Chemometric assessment of soil pollution and pollution source apportionment for an industrially impacted region around a non-ferrous metal smelter in Bulgaria. Molecules 24(5):883. https://doi.org/10.3390/molecules24050883
18. Kumar V, Sharma A, Kaur P, Sidhu GPS, Bali AS, Bhardwaj R, Thukral AK, Cerda A (2019) Pollution assessment of heavy metals in soils of India and ecological risk assessment: a state-of-the-art. Chemosphere 216:449–462. https://doi.org/10.1016/j.chemosphere.2018.10.066
19. Javaid A, Yousaf W, Ahmad SR, Qadir A (2020) Application of pollution indices for the assessment of heavy metal hazards in soil using GIS approach. Arab J Geosci 13(22):1212. https://doi.org/10.1007/s12517-020-06164-2
20. Pan F, Yu Y, Yu L, Lin HL, Wang YY, Zhang LL, Pan DW, Zhu RL (2020) Quantitative assessment on soil concentration of heavy metal-contaminated soil with various sample pretreatment techniques and detection methods. Environ Monit Assess 192(12):800. https://doi.org/10.1007/s10661-020-08775-4
21. Tepanosyan G, Maghakyan N, Sahakyan L, Saghatelyan A (2017) Heavy metals pollution levels and children health risk assessment of Yerevan kindergartens soils. Ecotoxicol Environ Saf 142:257–265. https://doi.org/10.1016/j.ecoenv.2017.04.013
22. Yu S, Yun ST, Hwang SI, Chae G (2019) One-at-a-time sensitivity analysis of pollutant loadings to subsurface properties for the assessment of soil and groundwater pollution potential. Environ Sci Pollut Res 26(1):21216–21238. https://doi.org/10.1007/s11356-019-05002-7
23. Zhou CH, Liu CQ, Liang JH, Wang SH (2018) Numerical simulation of pollutant transport in soils surrounding subway infrastructure. Environ Sci Pollut Res 25(7):6859–6869. https://doi.org/10.1007/s11356-017-0968-0
24. Cao J, Xie CY, Hou ZR (2021) Transport patterns and numerical simulation of heavy metal pollutants in soils of lead-zinc ore mines. J Mt Sci 18(9):2345–2356. https://doi.org/10.1007/s11629-021-6851-y
25. Luan HJ, Lin HL, Jiang YJ, Wang YH, Liu JK, Wang P (2018) Risks induced by room mining goaf and their assessment: a case study in the shenfu-dongsheng mining area. Sustainability 10(3):631. https://doi.org/10.3390/su10030631
26. Yurkevich NV, Abrosimova NA, Bortnikova SB, Karin YG, Saeva OP (2017) Geophysical investigations for evaluation of environmental pollution in a mine tailings area. Toxicol Environ Chem 99(9–10):1328–1345. https://doi.org/10.1080/02772248.2017.1371308
27. Islam N, Saikia BK (2020) Atmospheric particulate matter and potentially hazardous compounds around residential/road side soil in an urban area. Chemosphere 259:127453. https://doi.org/10.1016/j.chemosphere.2020.127453
28. Yu XY, Mu C, Zhang DD (2020) Assessment of land reclamation benefits in mining areas using fuzzy comprehensive evaluation. Sustainability 12(5):2015. https://doi.org/10.3390/su12052015
29. Lu XZ, Gu AQ, Huang CL, Wei YC, Xu MX, Yin HQ, Hu XF (2021) Assessments of heavy metal pollution of a farmland in an urban area based on the Environmental Geochemical Baselines. J Soils Sediments 21(7):2659–2671. https://doi.org/10.1007/s11368-021-02945-8
30. Singh KP, Mohan D, Sinha S, Dalwani R (2004) Impact assessment of treated/untreated wastewater toxicants discharged by sewage treatment plants on health, agricultural, and environmental quality in the wastewater disposal area. Chemosphere 55(2):227–255. https://doi.org/10.1016/j.chemosphere.2003.10.050
31. Ko MS, Nguyen TH, Kim YG, Linh BM, Chanpiwat P, Hoang HNT, Nguyen TAH, Tuyến LH, Bien NQ, Nguyen VA, Kim KW (2020) Assessment and source identification of As and Cd contamination in soil and plants in the vicinity of the Nui Phao Mine, Vietnam. Environ Geochem Health 42(12):4193–4201. https://doi.org/10.1007/s10653-020-00631-1
32. Buscaroli A, Zannoni D, Menichetti M, Dinelli E (2017) Assessment of metal accumulation capacity of *Dittrichia viscosa* (L.) Greuter in two different Italian mine areas for contaminated soils remediation. J Geochem Explor 182:123–131. https://doi.org/10.1016/j.gexplo.2016.10.001
33. Manna A, Maiti R (2018) Geochemical contamination in the mine affected soil of Raniganj Coalfield—a river basin scale assessment. Geosci Front 9(5):1577–1590. https://doi.org/10.1016/j.gsf.2017.10.011
34. Punia A, Siddaiah NS, Singh SK (2017) Source and assessment of metal pollution at khetri copper mine tailings and neighboring soils, Rajasthan, India. Bull Environ Contam Toxicol 99(5):633–641. https://doi.org/10.1007/s00128-017-2175-6
35. Ustaoğlu F, Tepe Y, Aydin H (2020) Heavy metals in sediments of two nearby streams from Southeastern Black Sea coast: Contamination and ecological risk assessment. Environ Forensics 21(2):145–156. https://doi.org/10.1080/15275922.2020.1728433
36. Varol M, Ustaoğlu F, Tokatlı C (2022) Ecological risks and controlling factors of trace elements in sediments of dam lakes in the Black Sea Region (Turkey). Environ Res 205:112478. https://doi.org/10.1016/j.envres.2021.112478
37. Cao J, Xie CY, Hou ZR (2022) Ecological evaluation of heavy metal pollution in the soil of Pb-Zn mines. Ecotoxicology. https://doi.org/10.1007/s10646-021-02505-3
38. He Y, Li BB, Zhang KN, Li Z, Chen YG, Ye WM (2019) Experimental and numerical study on heavy metal contaminant migration and retention behavior of engineered barrier in tailings pond. Environ Pollut 252:1010–1018. https://doi.org/10.1016/j.envpol.2019.06.072
39. Cockett R, Heagy LJ, Haber E (2018) Efficient 3D inversions using the Richards equation. Comput Geosci 116:91–102. https://doi.org/10.1016/j.cageo.2018.04.006
40. Tu TB, Ercan A, Kavvas ML (2020) Probabilistic solution to two-dimensional stochastic solute transport model by the Fokker-Planck equation approach. J Hydrol 580:124250. https://doi.org/10.1016/j.jhydrol.2019.124250
41. Rapant S, Krčmová K (2007) Health risk assessment maps for arsenic groundwater content: application of national geochemical databases. Environ Geochem Health 29(2):131–141. https://doi.org/10.1007/s10653-006-9072-y
42. Ustaoğlu F, Tepe Y (2019) Water quality and sediment contamination assessment of Pazarsuyu Stream, Turkey using multivariate statistical methods and pollution indicators. Int Soil Water Conserv Res 7(1):47–56. https://doi.org/10.1016/j.iswcr.2018.09.001
43. Antoniadis V, Shaheen SM, Boersch J, Frohne T, Du-Laing G, Rinklebe J (2017) Bioavailability and risk assessment of potentially toxic elements in garden edible vegetables and soils around a highly contaminated former mining area in Germany. J Environ Manage 186:192–200. https://doi.org/10.1016/j.jenvman.2016.04.036
44. Damptey FG, Birkhofer K, Nsiah PK, Riva EGDL (2020) Soil properties and biomass attributes in a former gravel mine area after two decades of forest restoration. Land 9(6):209. https://doi.org/10.3390/land9060209
45. Bokar H, Traore AZ, Mariko A, Diallo T, Traore A, Sy A, Soumare O, Dolo A, Bamba F, Sacko M, Toure O (2020) Geogenic influence and impact of mining activities on water soil and plants in surrounding areas of Morila Mine, Mali. J Geochem Explor 209(4):106429. https://doi.org/10.1016/j.gexplo.2019.106429
46. Pelica J, Barbosa S, Reboredo F, Lidon F, Pessoa F, Calvao T (2018) The paradigm of high concentration of metals of natural or anthropogenic origin in soils—the case of Neves-Corvo mine area (Southern Portugal). J Geochem Explor 186:12–23. https://doi.org/10.1016/j.gexplo.2017.11.021
47. Hu JJ, Lin BJ, Yuan MY, Lao ZL, Wu KM, Zeng YY, Liang ZH, Li HR, Li YL, Zhu D, Liu JL, Fan HB (2019) Trace metal pollution and ecological risk assessment in agricultural soil in Dexing Pb/Zn mining area, China. Environ Geochem Health 41(2):967–980. https://doi.org/10.1007/s10653-018-0193-x
48. Yevugah LL, Darko G, Bak J (2021) Does mercury emission from small-scale gold mining cause widespread soil pollution in Ghana? Environ Pollut 284:116945. https://doi.org/10.1016/j.envpol.2021.116945
49. Zhao YJ, Deng QY, Lin Q, Zeng CY, Zhong C (2020) Cadmium source identification in soils and high-risk regions predicted by geographical

detector method. Environ Pollut 263:114338. https://doi.org/10.1016/j.envpol.2020.114338
50. Romero-Baena AJ, González I, Galán E (2018) Soil pollution by mining activities in Andalusia (South Spain)—the role of Mineralogy and Geochemistry in three case studies. J Soil Sediments 18(6):2231–2247. https://doi.org/10.1007/s11368-017-1898-7
51. Tahmasebi P, Taheri M, Gharaie MHM (2020) Heavy metal pollution associated with mining activity in the Kouh-e Zar region, NE Iran. Bull Eng Geol Env 79(2):1113–1123. https://doi.org/10.1007/s10064-019-01574-3
52. Ustaoğlu F, Islam MS (2020) Potential toxic elements in sediment of some rivers at Giresun, Northeast Turkey: a preliminary assessment for ecotoxicological status and health risk. Ecol Ind 113:106237. https://doi.org/10.1016/j.ecolind.2020.106237
53. Tytła M (2019) Assessment of heavy metal pollution and potential ecological risk in sewage sludge from municipal wastewater treatment plant located in the most industrialized region in Poland—case study. Int J Environ Res Public Health 16(13):2430. https://doi.org/10.3390/ijerph16132430
54. Simiele M, Lebrun M, Del-Cioppo G, Scippa SG, Trupiano D, Bourgerie S, Morabito D (2020) Evaluation of different amendment combinations associated with trifolium repens to stabilize Pb and As in a mine-contaminated soil. Water Air Soil Pollut 231(11):539. https://doi.org/10.1007/s11270-020-04908-0
55. Zhang X, Yang HH, Cui ZJ (2018) Evaluation and analysis of soil migration and distribution characteristics of heavy metals in iron tailings. J Clean Prod 172:475–480. https://doi.org/10.1016/j.jclepro.2017.09.277
56. Maskall J, Whitehead K, Thornton I (1995) Heavy metal migration in soils and rocks at historical smelting sites. Environ Geochem Health 17(3):127–138. https://doi.org/10.1007/BF00126081
57. Jacques D, Šimůnek J, Mallants D, Van-Genuchten MT (2008) Modelling coupled water flow, solute transport and geochemical reactions affecting heavy metal migration in a podzol soil. Geoderma 145(3):449–461. https://doi.org/10.1016/j.geoderma.2008.01.009
58. Kakareka SV, Salivonchik SV (2017) Forecasting heavy metal pollution of soils in an administrative district of Belarus. Geograph and Nat Res 38(3):295–302. https://doi.org/10.21782/GIPR0206-1619-2017-3
59. Khan S, Khan NN, Iqbal N (1991) Studies on the effects of some organic pollutants on the heavy metal transport in an Indian soil. Environ Pollut 70(2):109–115. https://doi.org/10.1016/0269-7491(91)90083-9
60. Zhang YM, Li S, Lai YX, Wang LQ, Wang F, Chen Z (2019) Predicting future contents of soil heavy metals and related health risks by combining the models of source apportionment, soil metal accumulation and industrial economic theory. Ecotoxicol Environ Saf 171:211–221. https://doi.org/10.1016/j.ecoenv.2018.12.023
61. Hou DY, O'Connor D, Nathanail P, Tian L, Ma Y (2017) Integrated GIS and multivariate statistical analysis for regional scale assessment of heavy metal soil contamination: a critical review. Environ Pollut 231:1188–1200. https://doi.org/10.1016/j.envpol.2017.07.021
62. Ruiz-Fernández AC, Sanchez-Cabeza JA, Pérez-Bernal LH, Gracia A (2019) Spatial and temporal distribution of heavy metal concentrations and enrichment in the southern Gulf of Mexico. Sci Total Environ 651:3174–3186. https://doi.org/10.1016/j.scitotenv.2018.10.109
63. Liu ZC, Chen BN, Wang LA, Urbanovich O, Nagorskaya L, Li X, Tang L (2020) A review on phytoremediation of mercury contaminated soils. J Hazard Mater 400:123138. https://doi.org/10.1016/j.jhazmat.2020.123138
64. Chai L, Wang YH, Wang X, Ma L, Cheng ZX, Su LM (2021) Pollution characteristics, spatial distributions, and source apportionment of heavy metals in cultivated soil in Lanzhou, China. Ecol Indicat 125:107507. https://doi.org/10.1016/j.ecolind.2021.107507
65. Adimalla N (2020) Heavy metals contamination in urban surface soils of Medak province, India, and its risk assessment and spatial distribution. Environ Geochem Health 42(1):59–75. https://doi.org/10.1007/s10653-019-00270-1
66. Ding Q, Cheng G, Wang Y, Zhuang DF (2017) Effects of natural factors on the spatial distribution of heavy metals in soils surrounding mining regions. Sci Total Environ 578:577–585. https://doi.org/10.1016/j.scitotenv.2016.11.001
67. Černík M, Federer P, Borkovec M, Sticher H (1994) Modeling of heavy metal transport in a contaminated soil. J Environ Qual 23(6):1239–1248. https://doi.org/10.2134/jeq1994.00472425002300060017x
68. Merrington G, Alloway BJ (1994) The transfer and fate of Cd, Cu, Pb and Zn from two historic metalliferous mine sites in the UK. Appl Geochem 9(6):677–687. https://doi.org/10.1016/0883-2927(94)90027-2
69. Mishra J, Singh R, Arora NK (2017) Alleviation of heavy metal stress in plants and remediation of soil by rhizosphere microorganisms. Front Microbiol 8:1706. https://doi.org/10.3389/fmicb.2017.01706

Publisher's Note